Proceedings of IMECE2005
2005 ASME International Mechanical Engineering Congress and Exposition
November 5-11, 2005, Orlando, Florida USA

IMECE2005-79968

JOYSTICK ERGONOMIC STUDY IN MATERIAL HANDLING USING VIRTUAL HUMANS

Esteban Peña Pitarch
Universitat Politecnica de Catalunya
Departament Enginyeria Mecanica
Av. Bases de Manresa, 61-73
08240 Manresa, Spain
Tel: 0034-938-777266
Fax: 0034-938-777202
esteban.pena@upc.edu

Jingzhou Yang
The University of Iowa
Virtual Soldier Research Program
Center for Computer-Aided Design
111 Engineering Research Facility
Iowa City, IA 52242-1000

Karim Abdel-Malek
The University of Iowa
Virtual Soldier Research Program
Center for Computer-Aided Design
111 Engineering Research Facility
Iowa City, IA 52242-1000

Joo Kim
The University of Iowa
Virtual Soldier Research Program
Center for Computer-Aided Design
111 Engineering Research Facility
Iowa City, IA 52242-1000

Tim Marler
The University of Iowa
Virtual Soldier Research Program
Center for Computer-Aided Design
111 Engineering Research Facility
Iowa City, IA 52242-1000

ABSTRACT

Raw material and product manufacturing are related to material handling. Although there have been great advances in technologies, regulations, methodologies, strategies, and workplace safety, the number of fatalities, the severity of injuries, and the number of lost workdays per accident-incident related to material handling continue keeping high. Some hand injuries occur when the operators repetitively use joysticks to handle materials in manufacturing environment. This paper studies joystick ergonomics used in the material handling equipment and evaluates the design and use of joysticks using a new generation of virtual humans (Santos™). The Denavit-Hartenberg method is implemented to analyze the 25-degree-of-freedom (DOF) hand model of the virtual humans. Human performance measures (joint torques and joint displacements) are criteria for the design of joysticks in the material handling machines.

Keywords: Material handling, virtual humans, injuries, and grasping.

INTRODUCTION

The Virtual Soldier Research (VSR) program at The University of Iowa has developed a new generation, highly advanced virtual human (Santos™) capable of autonomously predicting postures and motions. Our virtual human can be developed to measure and monitor human performance indices such as physiological and musculoskeletal fatigue. The current success and momentum surrounding the development of Santos™ stems from VSR's ongoing work by its team of 36 researchers, including faculty, professional research staff, and graduate students. This effort, funded primarily by the US Army TACOM and various industry partners, is a multidisciplinary project built on the substantial expertise and experience of researchers in fields ranging from computer science to biomedical engineering.

This paper presents a general approach to evaluate the joystick design used in material handling. One of the criteria is to minimize joint torques in the hand.

There are various injuries related to material handling. Especially, when the operator repetitively uses the joystick for long time, the operator's hand will have problems. Therefore, to avoid this type of injury it is important to consider the ergonomic aspects of joysticks in the design stage.

The Santos'™ hand is a 25-DOF model [1] and the parametric length for each finger and bone is used [2]. In [3]

the same length was modified and adapt for simulated different tools.

Application of stable forces was applied in [4-8]. [9] proposed the programming robot by direct human demonstration. The Barrett hand [10] was used for grasping and manipulation. Grasp force was represented by the convex combination [11]. [12] presented fingers of a multi-fingered robot hand that touches an object. In [4] the hand is modeled with spherical sensors.

There are different studies that analyzed the forces for all the fingers when the hand grasps a cylinder or other objects [13-16]. However, to our knowledge, nobody has used mathematical hand model to guide joystick design.

This paper presents a new hand model to facilitate joystick ergonomic design. The nomenclature will first be introduced. Next the hand kinematic model is investigated. Finally, the strategy of hand grasping for a cylindrical object in virtual world is developed followed by the joint torque prediction to measure the design of the joystick.

NOMENCLATURE

J(**q**) : Augmented Jacobian matrix
f : Vector force
m : Vector moment
ℓ_{i-2} : Length proximal phalanx bone
ℓ_{i-3} : Length middle phalanx bone
ℓ_{i-4} : Length distal phalanx bone
q_j : Joint angle for joint *j*, where *j=1,…,25*
v : Translational velocity of the end-effector
$\boldsymbol{\tau}$: Torque vector
$\boldsymbol{\omega}$: Angular velocity of the end-effector frame

FORMULATION

Hand Model

The hand has 27 bones, where 8 small bones are distributed in the wrist, and the other 19 bones are distributed in the five fingers, depicted in Fig.1. Each finger has one metacarpal bone (the palm) and index, ring, middle and little fingers have three phalanxes (proximal, middle, distal) while the thumb has two phalanx (proximal and distal). The bones connect one with another via joints. There are two types of movement called troquelar (move in one direction) and condylar (move in two directions). This movement is similar to a hinge and has one DOF.

The symbolic Roman numbers are assigned for fingers: the thumb is I, the index finger is II, the middle finger is III, the ring finger is IV, and the little is V. At the base of each finger is one metacarpal bone, which connects to the wrist. Carpometacarpal (CMC) joints connect the metacarpal bones to the wrist. The CMC joints for II and III are static: they cannot actually rotate. In contrast, the CMC joints for I, IV, and V can rotate with Flexion/Extension (F/E) and Abduction/Adduction (Ab/Ad). The metacarpophalangeal (MCP) joints connect the metacarpal bones to the phalanx bones. These MCP joints also can move with 2 DOFs (F/E and Ab/Ad). An interphalangeal (IP) joint connects the two phalanx bones in the thumb and has one rotational degree of freedom. Proximal Interphalangeal (PIP) joints connect the two inner (not the tip) phalanxes in II, III, IV, and V. These joints have one rotational degree of freedom in the F/E direction. The last joint is the Distal Interphalangeal (DIP) joint. It connects the fingertips the final phalanxes in each of the fingers (II, III, IV, and V), and it moves in F/E direction.

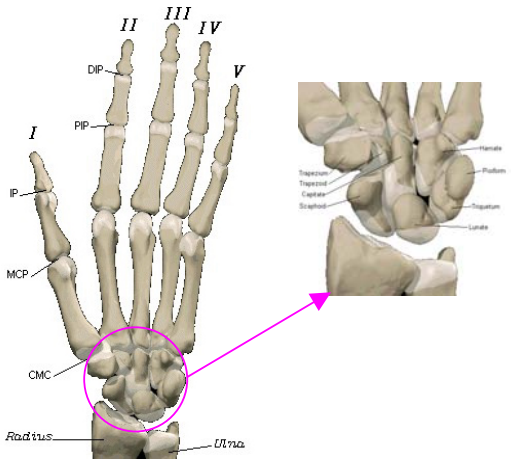

Fig.1. Palmar view of left hand bones

Figure 2 depicts the movements of F/E and Ad/Ab for one finger.

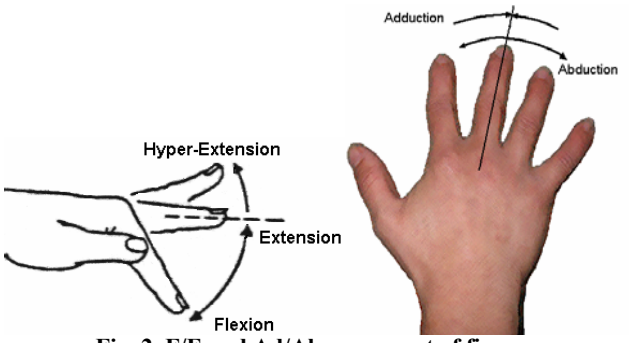

Fig. 2. F/E and Ad/Ab movement of fingers

To simulate the most realistic movement the hand model has 25 DOFs and the detail is shown in Fig.3.

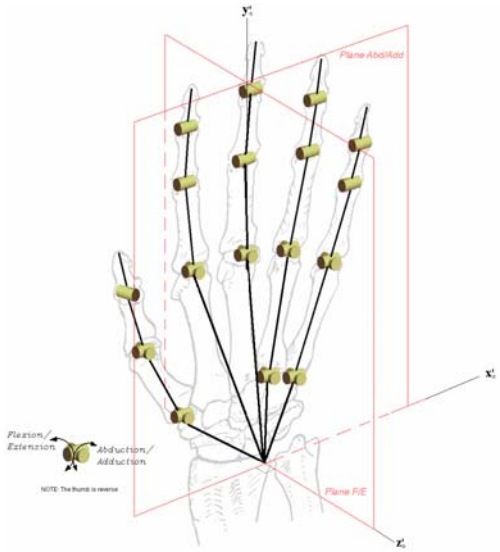

Fig. 3. Dorsal view right hand model

Strategy For Grasping Cylinder

Although there are many different ways to grasp a cylindrical object, the two major ones are grasping with power and grasping with precision. The task to grasp a pen from the table is one example for grasping with precision, while normally two fingers are involved in the grasping with the thumb and index in opposition. Of course, when one writes he/she can use two, three or four fingers.

Grasping a joystick is one example of grasping with power where normally four fingers (index, middle, ring and little) are involved in the grasping. Fig. 4 shows the configuration of this grasping.

Fig.5 depicts a schematic representation of fingers' positions except the thumb. When a person grasps a cylinder, in general, from observations the position of thumb stays in the neutral position. Furthermore, the proximal phalanx bones are tangential with the cylinder. Without lost generality, we assume the contact points are located in the middle of these bones. The length ℓ_{i-2} corresponds to the proximal phalanx bone where $i=II, III, IV, V$ which denotes index, middle, ring and little fingers, respectively. The length ℓ_{i-3} corresponds to the middle phalanx and the length ℓ_{i-4} denotes the distal phalanx.

Fig. 4. Virtual human grasp a cylinder

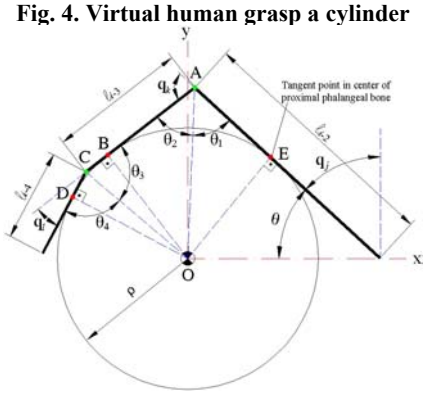

Fig. 5. Schematic finger grasping a cylinder

The lengths of different bones are from [2], [3] and shown in Table 1. The hand dimensions are shown in Fig. 6.

	Proximal		Middle		Distal	
Thumb	$0.196 * HL$	ℓ_{I-2}	–	–	$0.158 * HL$	ℓ_{I-3}
Index	$0.265 * HL$	ℓ_{II-2}	$0.143 * HL$	ℓ_{II-3}	$0.097 * HL$	ℓ_{II-4}
Middle	$0.277 * HL$	ℓ_{III-2}	$0.170 * HL$	ℓ_{III-3}	$0.108 * HL$	ℓ_{III-4}
Ring	$0.259 * HL$	ℓ_{IV-2}	$0.165 * HL$	ℓ_{IV-3}	$0.107 * HL$	ℓ_{IV-4}
Pinkie	$0.206 * HL$	ℓ_{V-2}	$0.117 * HL$	ℓ_{V-3}	$0.093 * HL$	ℓ_{V-4}

Table 1. Lengths for the phalanx bones

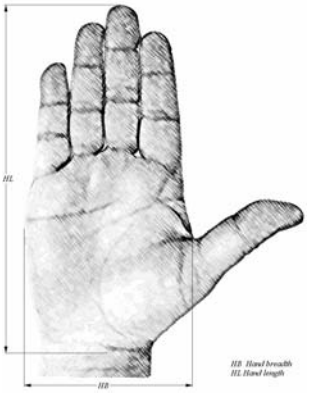

Fig. 6. Parametric hand

For a better design of joysticks the objective is to determine an optimal grasping position for the hand where fingers have minimum joint torques. From Fig.5 the finger configurations are related to the diameter of the cylinder. To use a joystick the thumb moves freely to reach or push the control buttons and the other four fingers can only move in F/E movements.

The joint angles involved in this grasping configuration for the index are q_7, q_8, q_9, q_{11}, q_{12}, q_{13} for the middle, q_{17}, q_{18}, q_{19} for the ring and q_{23}, q_{24}, q_{25} for the little.

In this study, we choose a series of radius ρ from 5 mm to 40 mm. According to these radii, we can calculate the joint angles in degrees shown in Tables 2, 3, 4, and 5.

INDEX			
ρ (mm)	q_7 (MCP)	q_8 (PIP)	q_9 (DIP)
5	79.32	100	45.56
10	69.32	100	23.72
15	60.49	100	15.94
20	52.96	100	11.99
25	46.67	93.37	9.6
30	41.45	82.91	8.00
35	37.13	74.26	6.87
40	33.52	67.05	6.01

Table 2. Joint angles for the index finger

MIDDLE			
ρ (mm)	q_{11} (MCP)	q_{12} (PIP)	q_{13} (DIP)
5	79.78	100	90
10	70.15	100	64.42
15	61.56	100	45.56
20	54.17	100	35.00
25	47.93	95.86	28.28
30	42.72	85.43	23.72
35	38.36	76.72	20.40
40	34.70	69.40	17.90

Table 3. Joint angles for the middle finger

RING			
ρ (mm)	q_{17} (MCP)	q_{18} (PIP)	q_{19} (DIP)
5	79.07	100	90
10	68.88	100	70.75
15	59.92	100	50.66
20	52.32	100	39.10
25	46.01	92.03	31.71
30	40.80	81.61	26.63
35	36.05	73.00	22.93
40	32.92	65.84	20.13

Table 4. Joint angles for the ring finger

LITTLE			
ρ (mm)	q_{23} (MCP)	q_{24} (PIP)	q_{25} (DIP)
5	76.36	100	58.50
10	64.10	100	31.28
15	53.94	100	21.14
20	45.85	91.70	15.94
25	39.49	78.97	12.78
30	34.47	68.95	10.664
35	30.48	60.95	9.15
40	27.25	54.50	8.00

Table 5. Joint angles for the little finger

For small radius cylinders the PIP joints reach their upper limits of motion, i.e. 100 degrees. The larger the radius the smaller the finger joints from the above joint angle tables.

To validate these angles we do the experiment shown in Figs.7-9 where a human hand grasps a cylinder with different radius.

Fig. 7. Grasping cylinder (radius 10 mm)

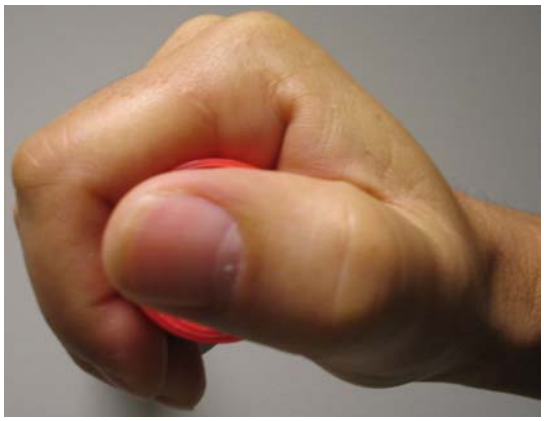

Fig. 8. Grasping cylinder (radius 15 mm)

Fig. 9. Grasping cylinder radius (25 mm)

Fig.7 shows an experiment that a human hand grasps a cylinder with radius 10 mm and the length of the cylinder bar 190 mm. From measurement q_7 is 69 degrees. Other angles are also close the calculated results. For other radii cylinders, the experiment results match ones calculated by the proposed strategy.

Fig. 10 shows one example that a human hand grasps a commercial joystick. From observation grasping joysticks is similar to grasping cylinders and the fingers' configuration is similar for both cases.

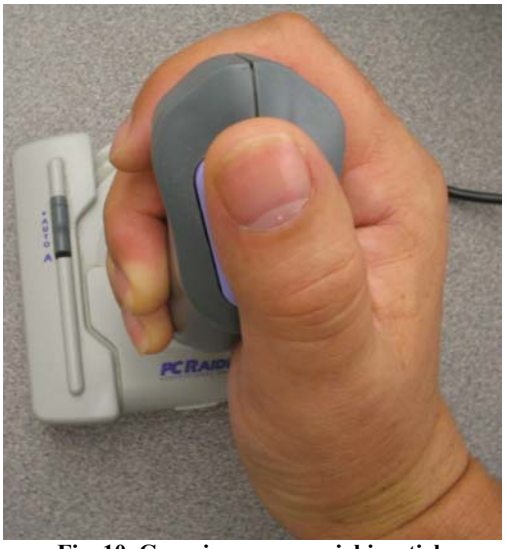

Fig. 10. Grasping commercial joystick

After the strategy of grasping for the joystick has been developed, the design of joysticks will depends on the joint torques in the fingers. In next section we will discuss joint torque formulation.

Finger Joint Torque

Since the hand grasping velocity and acceleration are small, we consider hand grasping as one static problem. Therefore, finger joint torques will be the general static torques.

From the time differentiation of the linear and angular position using the chain rule, we can obtain the linear relationship between the linear/angular velocity vector (in Cartesian space) and the joint velocity vector (in joint space) as follows:

$$\begin{bmatrix} \mathrm{v} \\ \omega \end{bmatrix} = \mathrm{J}(\mathrm{q})\dot{\mathrm{q}} \tag{1}$$

where $\mathbf{v}$ is the translational velocity of the end-effector and $\boldsymbol{\omega}$ is the angular velocity of the end-effector frame. $\mathbf{J}(\mathbf{q})$ is the augmented Jacobian matrix of the kinematic structure defined by

$$\mathbf{J}(\mathbf{q}) = \begin{bmatrix} \mathbf{J}_x \\ \mathbf{J}_\omega \end{bmatrix} \tag{2}$$

This also indicates that the virtual displacements have the similar relationship.

$$\begin{bmatrix} \delta\mathbf{x} \\ \delta\boldsymbol{\theta} \end{bmatrix} = \mathbf{J}(\mathbf{q})\delta\mathbf{q} \qquad \forall\delta\mathbf{q} \tag{3}$$

where $\delta\mathbf{x}$, $\delta\boldsymbol{\theta}$, and $\delta\mathbf{q}$ are the virtual displacement vectors of Cartesian linear, Cartesian angular, and joint, respectively.

We begin with the calculation of the torque at each joint. To account for all of the elements that enter into calculating the torque at a given joint, we apply the principle of virtual work to the two force systems. As for the joint torques, its associated virtual work is

$$\delta W_\tau = \boldsymbol{\tau}^T \delta\boldsymbol{q} \tag{4}$$

where δW is the virtual work. For the end-effector forces $\mathbf{F} = \begin{bmatrix} \mathbf{f}^T & \mathbf{m}^T \end{bmatrix}^T$, comprised of a force vector $\mathbf{f}$ and a moment vector $\mathbf{m}$, the virtual work performed is

$$\delta W_{\mathbf{F}} = \mathbf{f}^T \delta\mathbf{x} + \mathbf{m}^T \boldsymbol{\omega}\delta t \tag{5}$$

where $\delta\mathbf{x}$ is the linear virtual displacement and $\boldsymbol{\omega}\delta t$ is the angular virtual displacement of the end-effector, respectively. Because the difference between the virtual work of the joint torques and the virtual work of the end-effector forces shall be null for all joint virtual displacements, we write

$$\boldsymbol{\tau}^T \delta\boldsymbol{q} = \boldsymbol{F}^T \boldsymbol{J}(\boldsymbol{q})\delta\boldsymbol{q} \qquad \forall\boldsymbol{q} \tag{6}$$

The relationship between the joint torque vector and end-effector force/moment vector is then given by

$$\boldsymbol{\tau} = \boldsymbol{J}^T \boldsymbol{F} \tag{7}$$

where the torque vector is $\boldsymbol{\tau} = [\tau_1, \tau_2, ..., \tau_n]^T$.

Now, we extend this formulation to the case where multiple external loads (both translational and rotational) are applied to any location of any finger/link, not necessarily to the end-effector. Let's assume that a general form of external load $\mathbf{F}_k$ is applied to the point at ${}^k r_k$ location of finger segment k, where ${}^k r_k$ location vector is expressed with respect to k^{th} local coordinate frame.

This point of application of external load can be regarded as the end-effector for the corresponding external load. The augmented Jacobian matrix $\mathbf{J}_k$ for this point is derived from the linear relationship between the joint velocity vector and the Cartesian velocity vector:

$$\mathbf{J}_k(\mathbf{q}) = \begin{bmatrix} \dfrac{\partial {}^0\mathbf{T}_1(\mathbf{q})}{\partial q_1} {}^k\mathbf{r}_k & \cdots & \dfrac{\partial {}^0\mathbf{T}_i(\mathbf{q})}{\partial q_i} {}^k\mathbf{r}_k & \cdots & \dfrac{\partial {}^0\mathbf{T}_k(\mathbf{q})}{\partial q_k} {}^k\mathbf{r}_k \\ \mathbf{Z}_0(\mathbf{q}) & \cdots & \mathbf{Z}_{i-1}(\mathbf{q}) & \cdots & \mathbf{Z}_{k-1}(\mathbf{q}) \end{bmatrix}_{6\times k} \tag{8}$$

where $\mathbf{Z}_{i-1}, i = 1, ..., k$ is the local z-axis vector of joint i expressed in terms of the global coordinate system.

So the joint torque vector due to the external load applied at point ${}^k r_k$ of link k is

$$\boldsymbol{\tau}_k = \boldsymbol{J}_k^T \boldsymbol{F}_k \tag{9}$$

From the principle of superposition, the total joint torques due to several external loads are obtained as a sum of all joint torques:

$$\boldsymbol{\tau} = \sum_k \boldsymbol{J}_k{}^{\mathbf{T}} \boldsymbol{F}_k \tag{10}$$

RESULTS

A 95% percentile of people that has the hand with length (HL) 190 mm and hand breadth (HB) 90 mm is considered as the given input. From Table 1, we can obtain the lengths of all segments of the fingers. The cylinder with a radius ρ from 5 mm to 40 mm is used to determine the joint torques. For cylinders with radii that are larger than 40 mm, it needs two hands to grasp together for A 95% percentile of people.

Using the above section formulations we obtain the joint torques for all fingers. Fig. 11 shows the summation of joint torques for each finger and the larger the radius is, the larger the torque is when we apply the same hand contact forces with the object. The result suggests that we should choose smaller radius for the joystick. However, The smaller the radius is, the larger joint displacements are with respect to the neural gesture of the hand shown in Table 6.

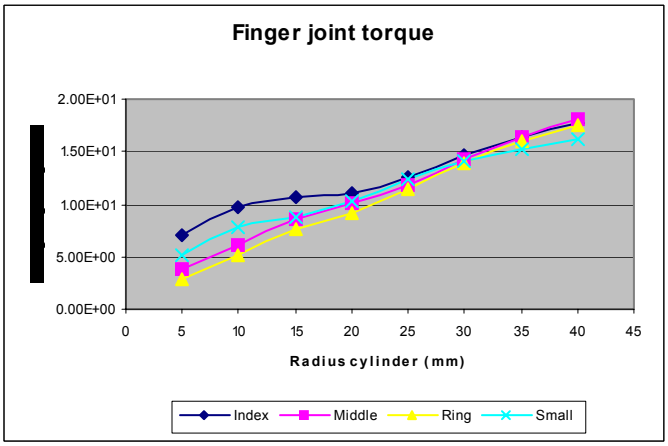

Fig. 11. Fingers joint torque

Neutral gesture of the hand				
Thumb	Index	Middle	Ring	Little
q_1 =0	q_6 =0	q_{10} =0	q_{14} =0	q_{20} =0
q_2 =0	q_7 =30	q_{11} =30	q_{15} =2	q_{21} =5
q_3 =30	q_8 =30	q_{12} =30	q_{16} =0	q_{22} =0
q_4 =0	q_9 =10	q_{13} =10	q_{17} =30	q_{23} =30
q_5 =30			q_{18} =30	q_{24} =30
			q_{19} =10	q_{25} =10

Table 6 Angles for the neutral gesture of hand (in degrees)

Therefore, the suggested radius for the middle finger should be 15 mm-20 mm. And the radii for other fingers are little bit smaller than 15 mm.

CONCLUSIONS

Virtual human hand grasping is proposed for joystick ergonomic design. Santos™ is a 101-DOF digital human model with 25 DOFs for each hand. Based on the hand model a grasping strategy is developed and joint torques are calculated to evaluate the design of joysticks in material handling machines. The experiment results illustrate the validity of the proposed grasping strategy for cylindrical objects. Human performance measures such as joint torques and joint displacements are the criteria to give the feedback from the virtual hands to test the design.

ACKNOWLEDGMENTS

This research was funded by the U.S. Army project "Digital Humans and Virtual Reality for Future Combat Systems" (Contract No.: DAAE07-03-D-L003).

REFERENCE

[1] Pena-Pitarch, E., Yang, J., and Abdel-Malek, K., 2005 "SANTOS™ Hand: A 25 Degree-Of-Freedom Model", *SAE International,* Iowa City, IA, June 14-16, 2005-01-2727 DHM.
[2] Buchcholz, B., Armstrong, T.J., and Goldstein, S.A., 1992, "Anthropometric data for describing the kinematics of the human hand", Ergonomics, 35(3), 261-273.
[3] Sancho-Bru, X., 2000, "Model biomecanic de la ma orientat al disseny d'eines manuals*",* PhD Dissertation, Universitat Jaume I, Castello (Spain), Gener.
[4] Yu,Y., Li,Y., & Tsujio,S., 2001, "Analysis of Finger Position Regions on Grasped Object with Multifingered Hand", Proc. 4th IEEE International Symposium on Assembly and Task Planning Soft Research Park, Fukuoka, Japan, 178-183.
[5] Howard, W.S. & Kumar, V., 1996, "On the Stability of Grasped Objects", IEEE Transactions on Robotics and Automation, *12*(6), 904-917.
[6] Zhu, X. & Wang, J., 2003, "Synthesis of Force-Closure Grasps on 3-D Objects Based on the Q distance", IEEE Transactions on Robotics and Automation, *19*(4), 669-679.
[7] Ponce, J. & Faverjon, B., 1995, "On Computing Three-Finger Force-Closure Grasp of Polygonal Objects", IEEE Transactions on Robotics and Automation, *11*(6), 868-881.
[8] Svinin, M.M., Ueda, K. & Kaneko, M., 1999, "On the Stability of an Object in Multi-Finger Grasping", Proc. Of the 1999 IEEE/RSJ International Conference on Intelligent Robots and Systems, 412-417.
[9] Kang, S.B. & Ikeuchi, K., 1997, "Toward Automatic Robot Instruction from Preception-Mapping Human Grasps to Manipulator Grasps", IEEE Transactions on Robotics and Automation, 13(1), 81-95.
[10] Liu, Y., Starr, G. , Wood, J. & Lumia, R., 2005, "Spatial grasp synthesis for complex objects using model-based simulation", Industrial Robot: An International Journal, 32/1, 24-31.
[11] Ding, D., Liu, Y.H. & Wang, S., 2001, "Computation of 3-D Form-Closure Grasps", IEEE Transactions on Robotics and Automation, 17(4), 515-522.
[12] Kaneko, M. & Tanie, K., 1994, "Contact Point Detection for Grasping an Unknown Object Using Self-Posture Changeability", IEEE Transactions on Robotics and Automation, 10(3), 355-367.
[13] Lee, J.W. & Rim, K., 1991, "Measurement of finger joint angles and maximum finger forces during cylinder grip activity", J. Biomed. Eng., 13, 152-162.
[14] Pollard, S.N., 2004, "Closure and quality equivalence for efficient synthesis of grasp from examples", The International Journal of Robotics Research, 23(6), 595-613.
[15] Freund, J., Toivonen, R. & Takala, E.-P., 2002, "Grip forces of the fingertips", Clinical Biomechanics", 17, 515-520.
[16] Kong, Y.-K., Freivalds, A. & Kim, S.E.,2004, "Evaluation of handles in a maximum gripping task", Ergonomics, 47(12), 1350-1364.